Scientia Iranica A (2022) 29(6), 2837–2849

Sharif University of Technology
Scientia Iranica
Transactions A: Civil Engineering
http://scientiairanica.sharif.edu

Design of steel wire loop connection for precast reinforced concrete structural components

S. Singhal[a,b], A. Chourasia[a,b,*], Y. Kajale[c]

a. *Academy of Scientific and Innovative Research (AcSIR), Ghaziabad - 201002, India.*
b. *CSIR-Central Building Research Institute, Roorkee - 247667, Uttarakhand, India.*
c. *Department of Planning and Design, BG Shirke Construction Technology Pvt. Ltd., Pune - 411036, Maharashtra, India.*

Received 3 January 2021; received in revised form 19 March 2021; accepted 31 January 2022

KEYWORDS
Loop connection;
Steel wire ropes;
Precast components;
Design methodology;
Numerical analysis.

Abstract. Loop connection for precast Reinforced Concrete (RC) structural components using U-bars is advocated by researchers on the grounds of simple mechanism and strength. However, the system is difficult to materialize on-site in the lieu of which U-bars may be replaced with steel wire ropes, which offer a more suitable system in terms of convenience during the installation process. However, the literature is not rich on design requirements and methodology for loop connection. Thus, a theoretical study was undertaken to formulate the design methodology for the loop connection formed using steel wire ropes. The behavior of loop connection is governed by tension and shear, influenced by characteristics of wire ropes, grout, and vertical transverse bar. A design example is illustrated for the loop connection between precast wall-columns and the corresponding validation is demonstrated through numerical analysis and performance comparison with monolithic system and U-bar connection. The advantage of this research lies in the application of the systematic design approach with emphasis on all the influencing parameters of steel wire loop connection for precast components. It is expected that practicing engineers find the proposed design methodology useful in designing the loop connection for precast components.

1. Introduction

Seismic performance of precast structures has been a matter of investigation since a couple of decades ago. Precast buildings have witnessed significant damage during the previous earthquakes, which mainly concentrate around the joint regions, owing to the incompetent connection systems that tend to loosen during the ground motion [1]. Inadequate anchorage between the precast Reinforced Concrete (RC) components was found to be the main source of damage in several earthquakes worldwide. The structural behavior of precast structural components is dominated by the mechanism and strength of joint connections, demanding adequate load transfer and ductility. Often, joints between precast RC components are provided with grout and without any mechanical connection, thus leading to discontinuity between the precast panels and affecting structural performance due to partial load transfer [2–4]. Thus, mechanical connection is inevitable to achieve the monolithic behavior of the precast RC system. The

*. *Corresponding author.*
E-mail addresses: shubham@cbri.res.in (S. Singhal); ajayc@cbri.res.in (A. Chourasia); ypkajale@shirke.co.in (Y. Kajale)

doi: 10.24200/sci.2022.57459.5252

reinforcement of precast RC components sometimes acts as a mechanical connection itself, wherein rebars of two precast components are connected on-site [5].

Dowel bars are prevalent in the construction industry and are widely used as a connection for precast panels, where reinforcing bars are protruded from one panel and inserted into the sleeves provided in another panel [6]. However, dowel bars require a large embedment length, which otherwise leads to shear slip, early crushing, and rebar breakout during higher loading as observed in the studies of Ashok et al. [7] and Pramodh et al. [8]. El-desoqi et al. [9] conducted a progressive collapse assessment of precast RC beam-columns connected with reinforcement bars. Performance of dowel bars may be enhanced by attaching a steel head anchor at the end of reinforcing bars, known as the headed bar connection. Headed bars require less embedment depth and are capable of providing an adequate bond with the precast RC element [10]. Their bond strength may be enhanced further by providing grooves or ribs on the head surface [11]. Several connection systems for vertical joints have been recommended by researchers across the globe such as U-bars, O-connectors [12], steel plates and anchors [13], and U-shaped channel and rubber [14]. Table 1 summarizes different connection systems for precast RC panels and their behavior under lateral loading. Steel wire loop connection provides a robust joint, attracting the attention of researchers in the past decade. Joergensen and Hoang [15] conducted tests to investigate the effect of spacing between the loops, overlapping length of U-bars, and diameter of transverse rebar in the U-bar loop connection. Based on experimental results, the upper bound plasticity model was presented for loop connection using U-bars in the horizontal joint. Jørgensen and Hoang [16] studied the behavior of the loop connection under combined bending and tension loading. Rossley et al. [17] experimentally investigated the performance of the loop connection using U-bars for precast walls under lateral load. The main influencing parameters included concrete strength, diameter of transverse bar, and embedment depth of bars. In another study, an expression was proposed in the case of the strength of loop connection U-bars based on strut and tie theory [18]. Sørenson et al. [19] conducted an experimental investigation to evaluate the tensile capacity of loop connection and discussed the upper-bound solution based on the observed failure mechanism. Biswal et al. [20] studied the shear behavior of precast wall-to-wall joints with a loop connection using steel wire ropes with the objective of developing an empirical expression for shear load versus slip. The related literature reports research on tensile and shear behavior of the loop connection, but lacks a systematic approach to its design. Keeping the above in mind, this study presents a design philosophy based on tension in the loop bars and shear transfer along the joint, addressing all the design requirements and influencing parameters. The proposed design methodology is illustrated with a design example for precast RC walls and columns connected through loop connection. Consequently, a numerical analysis for the designed loop connection for precast RC wall and column is carried out for design validation. In addition, a comparison of the intended performance and those of monolithic system and similar U-bar connections is made.

2. Research significance

Loop connection for precast RC structural components offers various advantages with regard to its ease of installation, high flexibility, and strength. Despite the merits, wide acceptance of loop connection is limited in the construction industry owing to the lack of design methodology in the literature. A few available design philosophies in the literature include empirical upper-bound solutions based on experimental observations and results, which do not consider every factor influencing the behavior and strength of the loop connection. However, the effect of influencing parameters of loop connection cannot be ignored in a detailed assessment and also, in deciding on design requirements. Accordingly, our research objectives are to devise a design procedure for loop connection, which is validated through a finite element model, and to compare its performance with those of similar U-bar connections and monolithic systems. The proposed design procedure may be adopted by structural designers for designing a loop connection between vertical joints of precast RC components.

3. U-bar versus loop connection using steel wire ropes

U-bar is a widely investigated joint connection system where steel reinforcing bars in the shape of U are protruded from the adjacent panels and overlapped. A vertical interlocking bar (transverse bar) is inserted between the cores formed, or already embedded in raft prior to the placement of loops, to protrude till the full height of the panel. The joint is filled with the grout or concrete. U-bars have exhibited satisfactory performance under tensile loading, as reported in the relevant literature. However, apart from structural performance, it is indispensable to look into practical aspects and challenges during the implementation of a feasible solution. U-bar is subject to some drawbacks in terms of site installation, limiting its vast acceptance in the construction industry. In actual practice, it is required to install precast walls as vertical drop-down placement rather than horizontal installation. This practice is possible if the overlapping U-bars are bent

Table 1. Summary of connection systems for precast RC panels.

Authors	Connection system and joint	Connection description	Behavior under lateral loading
Pramodh et al. [8]	Dowel bars for wall-wall (vertical joint)	3–16 mm rebars embedded into the adjacent panel with an embedded length equal to development length	Joint separation due to shear slip and tensile stresses in dowel bars
Sritharan et al. [12]	O-connector for wall-column joint	Post-tensioned wall and column of the same thickness connected using 5 pairs of oval-shaped steel connectors	Dissipated energy by flexural yielding along the loading plane
Brunesi et al. [13]	Steel plates and anchors for wall-wall (vertical joint)	Steel bolts or anchors embedded in concrete through stud welded bars	Shear buckling failure, concrete crushing at base. Low energy dissipation, strength, and stiffness
Vaghei et al. [14]	U-shaped channel for wall-wall (horizontal and vertical joint)	Steel U-shaped channels attached to side of walls and tied together as male-female joints through nuts and bolts. U-shaped rubber implemented between two channels in order to dissipate vibration effect in structure	Adequate flexibility lateral strength, deformation capacity, and energy dissipation
Rossely et al. [17]	U-shape loop bars for wall-wall (horizontal joint)	High-strength loop bars protruding from precast panels and connected through lap splicing, longitudinal transverse bar inserted between the loop and joint filled with concrete	Concrete crushing at the joint; walls demonstrated brittle failure
Biswal et al. [20]	Loop connection for wall-wall (vertical joint)	U-bars or looped wires from adjacent panels overlapped with the vertical bar placed between the overlap	Shear capacity increased with decrease in loop bar spacing
Jørgensen et al. [21]	Loop connection for mutually perpendicular walls	Looped wire ropes from precast elements overlapped, forming a circular core	Rupture of wire ropes in T-connections at lower mortar strength
Peng et al. [22]	Sleeve with infusion pipe for wall-wall (horizontal joint)	Longitudinal bars from lower and upper wall panels inserted into sleeves and mortar poured into sleeve through infusion duct	Effective in transferring tensile stresses. Low deformation as compared to monolithic wall
Qiong et al. [23]	Sleeve connection for wall-wall (horizontal joint)	Longitudinal bars from wall panels inserted into sleeves and overlapped along with grouting	Similar energy dissipation as compared to cast-in-situ wall
Li et al. [24]	Vertical seam for wall-wall (horizontal joint)	Vertical joint having 10Φ@150 mm as strengthening reinforcement along height of the wall, joint filled with cement-sand mortar	Better energy dissipation as compared to monolithic wall
Sun et al. [25]	H-connector for wall-wall (horizontal joint)	H-shaped steel segment placed at the interface of walls and connected to walls through high-strength bolts	Favorable ductility and deformation capacity
Wang et al. [26]	Reinforcing bars and steel plates for wall-wall (horizontal joint)	Longitudinal rebars from precast wall welded to corresponding connecting steel plate, layer of high-strength mortar casted on top of lower wall plate, steel plates of lower wall inserted into the reserved channel at bottom of the upper wall, bolts inserted in aligned holes	No significant damage in the wall

Table 1. Summary of connection systems for precast RC panels (continued).

Authors	Connection system and joint	Connection description	Behavior under lateral loading
Guo et al. [27]	Steel plate and bars for wall-slab joint	Steel plate anchored with 6 and 8 mm diameter steel bars and 12 mm diameter high-strength steel bolts	Loosening of high-strength bolts, sliding of panels cracking
Li et al. [28]	Post-tensioning strands (wall-footing)	Precast panels stacked along horizontal joints, post-tensioning strands placed inside ungrouted ducts to connect panels to the foundation	Lower damage and self-centering capacity of precast post-tensioned walls

up prior to installation. However, when the diameter of U-bars is larger than 10 mm, bending and then again straightening of U-bars during the installation do not represent a viable and practical solution. Alternatively, reinforcing bars may be replaced with high-strength steel wire ropes to form a closed loop, which has a similar load transfer mechanism to that of U-bar and eliminates the shortcomings of the latter. Steel wire ropes are pre-manufactured, which are inserted in a steel wire box and embedded into the precast component, as shown in Figure 1. Loop connection using steel wire ropes comes with easy installation due to its high flexibility and no bending stiffness. Moreover, steel wire ropes have a much higher tensile strength, usually greater than 1500 N/mm^2, while the same for U-bars formed using reinforcing bars with the tensile strength of 415 N/mm^2 or 500 N/mm^2. In spite of their higher strength, steel wire ropes do not compromise on economy due to their comparatively lower diameter and less embedment depth requirement. Joints with concrete result in crushing and brittle failure during seismic loading. Thus, for damage limitation, it is recommended that the joint be filled with high-strength non-shrinkable grouting powder, ensuring free flow and higher degree of contact with precast panels, although the grouting powder is beneficial for joints up to 100 mm thick, above which concreting is preferable.

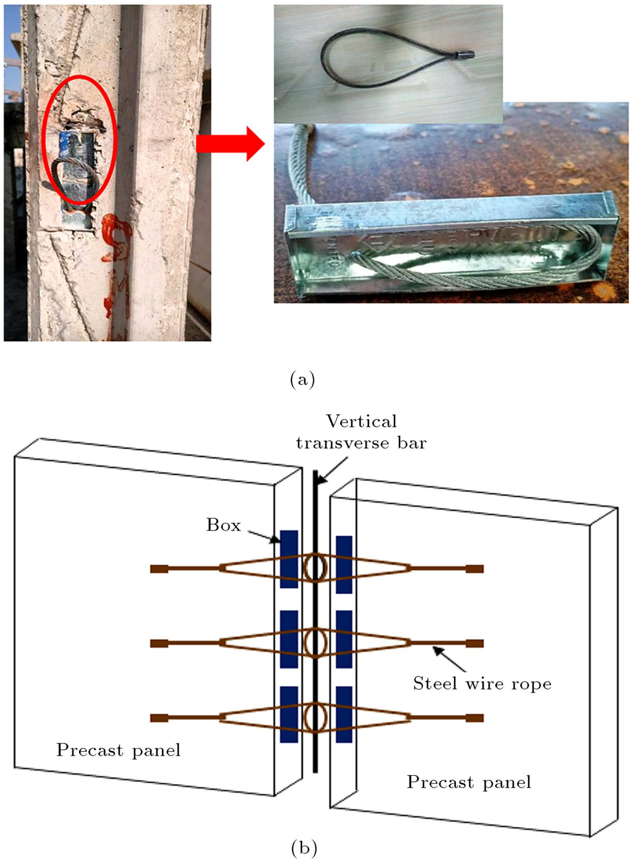

Figure 1. (a) Steel wire ropes inserted in wire box and embedded in the precast wall. (b) Schematic diagram of the joint.

4. Design and mechanism of loop connection

Designing of precast RC components can be done in a way similar to that of monolithic RC components as stipulated in various design codes and standards. Nevertheless, connections should be robust enough for an emulative monolithic system and must properly address tension, shear, deformation, and seismic resistance. In this respect, this section presents the design approach and safety checks for loop connection, which takes into consideration all the parameters that can influence the behavior of the connection. The parameters include anchorage length, strength of grout and steel wire ropes, spacing of loops, dimensions of precast panel and joint, diameter of steel wire ropes and vertical transverse bar, type of joint surface, and seismic load. Since the steel wire ropes have high tensile strength, usually more than 1500 N/mm^2, it is assumed that the failure would be governed by the yielding of vertical transverse bar or grout in the joint. The steel ropes behave as the strongest associate in the connection system. Shear along the vertical joint and compression is resisted by the grout in the joint, while the steel wire ropes and transverse bar will bear the tension developed in the joint.

4.1. Anchorage length of loop connection

Anchorage length is the length of steel wire ropes that is required to be embedded into precast RC components for an adequate anchorage or bond. Thus, design anchorage length is a function of bond strength of concrete and yield strength of steel wire ropes. Bond strength or bond stress acts at the interface of steel wire ropes and surrounding concrete, when steel wire is pulled by a tensile force T, as shown in Figure 2.

Maximum tensile force that can act on steel wire rope before the yield is given by Eq. (1) as follows:

$$T = \sigma_w \pi \frac{\phi_w^2}{4}, \tag{1}$$

where T = maximum tensile force acting on the steel wire rope; σ_w = yield strength of steel wire; and ϕ_w = diameter of steel wire.

To resist this force T, a resisting force T_{res} will develop depending on the anchorage length and the bond between steel wire and concrete. Since the steel wire ropes are bent into the loop fashion, the length is taken as twice. T_{res} is given by Eq. (2) as follows:

$$T_{res} = \tau_{bd} \pi \phi_w 2L, \tag{2}$$

where T_{res} = resisting force; τ_{bd} = bond stress as per Eq. (3); and L = anchorage length. Design bond stress or bond strength of concrete as per BS 8110:1997 [29] is:

$$\tau_{bd} = 1.4\beta\sqrt{f_{ck}}, \tag{3}$$

where β = bond coefficient as per BS 8110:1997 [29] and f_{ck} = compressive strength of precast concrete. β is dependent on the type of bond formed between steel and concrete, which may be taken as 0.65 for steel wire ropes as per BS 8110:1997 [29].

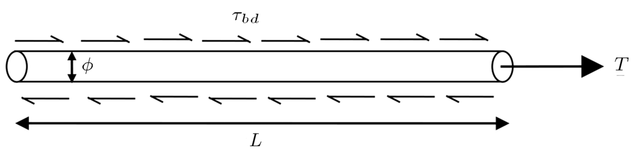

Figure 2. Bond stress and acting tensile load on steel wire rope.

For equilibrium, two forces (maximum tensile force and resisting force) shall be equated as shown in Eq. (4):

$$\sigma_w \pi \frac{\phi_w^2}{4} = \tau_{bd} \pi \phi_w 2L. \tag{4}$$

Thus, the anchorage length of loop can be determined using Eq. (5) as:

$$L = \frac{\sigma_w \phi_w}{8\tau_{bd}}. \tag{5}$$

Eq. (5) yields a slightly conservative value for the anchorage length. Alternatively, the anchorage length may be determined in accordance with DIN 1045 [30] as Eq. (6):

$$L = \frac{\alpha \sigma_w \phi_w}{7\tau_{bd}}, \tag{6}$$

where $\alpha = 0.7$ for loop in tension as per DIN 1045 [30].

4.2. Tensile capacity

Steel wire ropes are subjected to tension during the application of load. Since the wire ropes have very high tensile strength and a relatively low cross-sectional area (usually 6 mm diameter) with the loop forming a diameter in the range of 40–80 mm, these features result in high bearing stresses induced inside the loop/core region, which may result in cracks and local crushing in the grout confined within the loop. Load transfer in the loop connection occurs through bond stress and radial stress (Figure 3), which transfers into the surrounding mortar or grout due to compression or tension mechanism. The radial induced stresses result in the inclination of compressive struts, transferring the forces from one precast panel to another. Transverse reinforcement is responsible for resisting tension, which otherwise could result in splitting of grout in the plane of loop. The tension in steel wire rope must be counter-balanced with the radial stresses induced in the confined grout. An equilibrium condition is required to balance the tension in the steel wire rope, which is given by Eq. (7) or Eq. (8) as follows:

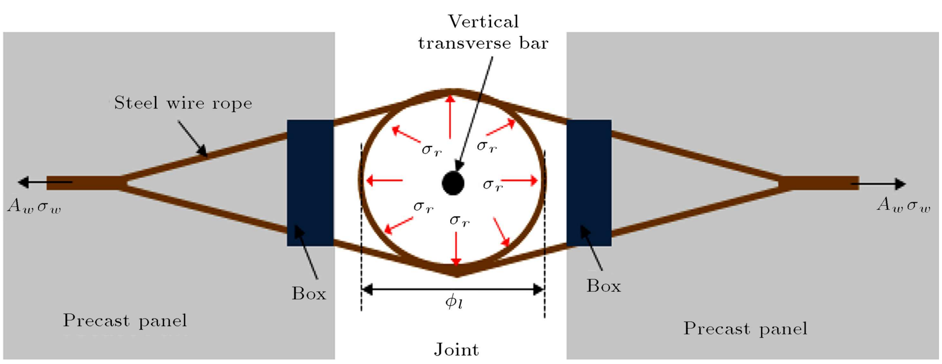

Figure 3. Loop connection showing radial stresses within loop.

$$\sigma_r \phi_l \phi_w = 2A_w \sigma'_w, \tag{7}$$

or:

$$\sigma_r = \frac{\pi \phi_w}{2\phi_l} \sigma'_w, \tag{8}$$

where σ_r = radial stress; ϕ_l = diameter of loop; A_w = cross-sectional area of steel wire ropes; and σ'_w = tensile stress acting on steel wires. However, the permissible radial stress based on the concept presented by Basler and Witta [31] may be determined as follows:

$$\sigma_{rp} = \sigma_g \sqrt{\frac{2c' + \phi_w}{\phi_w}}, \tag{9}$$

where σ_{rp} = permissible radial stress; σ_g = compressive strength of the grout, and c' = covering steel wire rope from the edge. Thus, the minimum tensile stress of steel wires is given by Eq. (10), which shall be limited by tensile strength of steel wire ropes, as conditioned in Eq. (11):

$$\sigma'_w = \frac{2\sigma_{rp}\phi_l}{\pi \phi_w}, \tag{10}$$

$$\sigma'_w < \sigma_w. \tag{11}$$

4.3. Shear capacity

Vertical joint between precast components experiences shear force along the joint interface. Shear capacity of the joint depends on the friction between the grout in joint and precast panel, tensile strength of grout, yield strength and diameter of steel wire ropes, and dimensions of the joint. Under shear loading, the joint has the tendency to experience vertical slip or torsion, which may cause separation and widening of the joint gap. To limit this phenomenon, it is required that sufficient anchorage be provided, which is ensured by the adequate number of steel wire ropes, along with appropriate embedment depth or anchorage length in the precast concrete, as illustrated in Section 4.1. Steel wire ropes will experience tension during separation in the joint due to shear slip, which should be balanced by equivalent compression in the grout. For equilibrium, compressive stresses generated in the joint grout may be given as Eq. (12):

$$\sigma_{cg} = \frac{2A_w}{A_c} \sigma_w, \tag{12}$$

where σ_{cg} = compressive stress generated in grout and A_c = area of the confined grout. Compressive stress affects the shear resistance of the joint and thus, must be considered to evaluate the shear resistance.

Design shear stress along the vertical joint may be computed using Eq. (13) as follows:

$$\tau_{des} = \frac{V}{wz}, \tag{13}$$

where τ_{des} = design shear stress; V = transverse shear force; w = width of the joint; and z = lever arm of the precast panel.

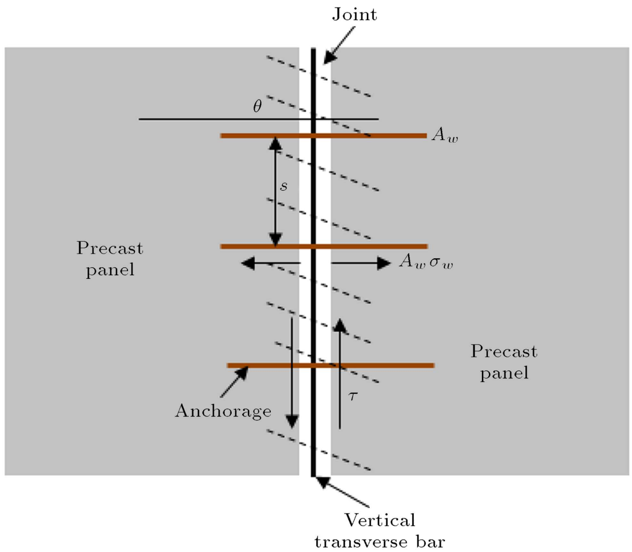

Figure 4. Shear mechanism at the joint interface.

The combined action of shear in the interface between precast panels and tension in steel wire ropes results in inclined compressive struts along the joint. Simultaneously, there will be an increase in compressive stress along the joint interface, which may lead to the crushing of grout at higher stresses. Consequently, the interface at the joint is subjected to shear due to friction and self-induced compressive stresses. Thus, the amount of steel along the joint must be sufficient to counter the inclined compressive struts and to enhance the shear capacity of the connection, which may be achieved by increasing the diameter or number of steel wire ropes. Therefore, this model determines the maximum amount of steel along the joint required to withstand the shear and compression. Figure 4 shows the mechanism of shear force along the joint interface.

When the joint grout and steel wire ropes both reach the plastic phase, a vertical equilibrium is established [32], which can be expressed in the form of Eq. (14) as follows:

$$(\sigma_g - \sigma_{cg}) t s \sin^2 \theta = \sigma_w \frac{\pi \phi_w^2}{2}, \tag{14}$$

where t = thickness of joint; s = spacing between steel wire ropes; and θ = angle of inclination strut, which is a function of frictional angle (ϕ_f) and may be determined as $90^\circ - \phi_f$.

During the plastic behavior of steel wire ropes and grout, the upper limit of shear stress or shear resistance for equilibrium (horizontal) is determined from Eq. (15) as:

$$\tau = (\sigma_g - \sigma_{cg}) \sin\theta \cos\theta. \tag{15}$$

It is recommended that a rough surface be provided for the joints with higher friction so that the angle of friction may be assumed between 30° and 50°. It is highly unlikely that steel wire ropes would reach their yield strength and it is expected that the failure is governed by grout in the joint, as stated earlier. Thus, this approach yields a highly conservative value of design shear resistance. In another approach consistent with EN 1992-1-1:2004 [33], design shear resistance along the joint can be determined using Eq. (16) as follows:

$$\tau = c\sigma_{tg} + \frac{\rho\sigma_w}{1.15}\mu, \tag{16}$$

where c = assumed to be 0.4 for rough surface and 0.2 for smooth surface; σ_{tg} = tensile strength of grout; ρ = steel ratio in the joint as per Eq. (17); and μ = assumed to be 0.7 and 0.6 for rough and smooth surfaces, respectively.

$$\rho = \frac{\pi\phi_w^2}{2ts}. \tag{17}$$

The following condition of Eq. (18) needs to be satisfied for shear force:

$$\tau > \tau_{des}. \tag{18}$$

For a viable loop connection system using steel wire ropes, tensile and shear capacities must be satisfied as conditioned in Eqs. (11) and (18).

4.4. Vertical transverse bar

Vertical interlocking transverse bar in the loop behaves as a tension member during the generation of tensile forces in steel wire ropes, leading to a push-and-pull action on the vertical bar during earthquake loading. The vertical transverse bar is required to be designed so that tension can be resisted, as is clear in Eq. (19), which adopts the maximum distortion criteria. Accordingly, the required area of transverse bar is given as follows:

$$A_v = \frac{A_w\sigma'_w\sqrt{3}}{f_y}, \tag{19}$$

where A_v = cross-sectional area of vertical transverse bar and f_y = yield strength of the vertical transverse bar.

Figure 5 depicts the flow chart illustrating the designing steps of the loop connection.

5. Design example

The design procedure presented in Section 4 is illustrated through a design example, wherein a precast RC wall is connected to precast RC columns through loop connection using steel wire ropes. The structural and geometrical details of the system correspond to the specimens being tested in an ongoing research program at the laboratory, where different connection systems for precast RC panels are tested.

5.1. Problem statement

The precast RC wall was measured by 1.01 m (L) $\times$ 2.26 m (H) $\times$ 0.30 m (W) with 0.35 m $\times$ 0.35 m precast columns at both ends, with a gap of 70 mm between wall and column components, thus having a total length of 1.85 m. The gap is filled with GP2 cement grout, having a compressive strength of 60 N/mm^2. Compressive strength of concrete is 30 N/mm^2, while that of reinforcement steel is 500 N/mm^2. The precast components are connected through loops of 6 mm diameter steel wires, having 1770 N/mm^2 tensile strength. Considering the gap between wall and column elements, it is feasible to form a 40 mm diameter loop for inserting a vertical transverse bar. Figure 6 shows the geometry and reinforcement of the precast RC wall-column system. The loop connection for the system is to be designed for a lateral load of 300 kN. Thus, f_{ck} = 30 N/mm^2, σ_w = 1770 N/mm^2, ϕ_w = 6 mm, σ_g = 60 N/mm^2, and c' = 15 mm. From Eq. (3), τ_{bd} = 4.98 N/mm^2. Anchorage or embedment length (L) for the steel wires is determined using Eq. (5) as 266 mm. Alternatively, Eq. (6) gives L = 213 mm. L = 213 mm is adopted for an economical design; permissible radial stress that may be experienced by the loop (Eq. (9)) is obtained by σ_{rp} = 147 N/mm^2; tensile stress is calculated by σ'_w = 624.20 N/mm^2 $<$ 1770 N/mm^2, which is acceptable as per the design"; and design shear stress as per Eq. (13) is obtained by τ_{des} = 1.15 N/ mm^2. Three pairs of steel wire ropes are provided equidistantly along the wall height. Thus, steel ratio in joint is ρ = 0.067%; and design shear resistance along the joint as per Eq. (16) is calculated by τ = 2.12 N/mm^2. Since, $\tau > \tau_{des}$, it is acceptable as per the design. Required cross-sectional area of the vertical transverse is bar = 183.32 mm^2. Thus, Fe500, 16 mm diameter rebar (200 mm^2) is provided as vertical transverse reinforcement.

6. Numerical analysis

Numerical analysis of precast RC wall-columns with the loop connection designed in Section 5 was carried out using Finite Element Analysis (FEA) package ABAQUS under displacement-controlled nonlinear static lateral loading until the load declined to 85% of the peak load.

6.1. Modeling approach

The objective of the study requires the numerical model to represent the non-linear response of concrete components for which explicit FEA technique is adopted that gives a solution through dynamic wave transmission in solid elements and does not require a fully assembled stiffness matrix, which involved complexity. Thus,

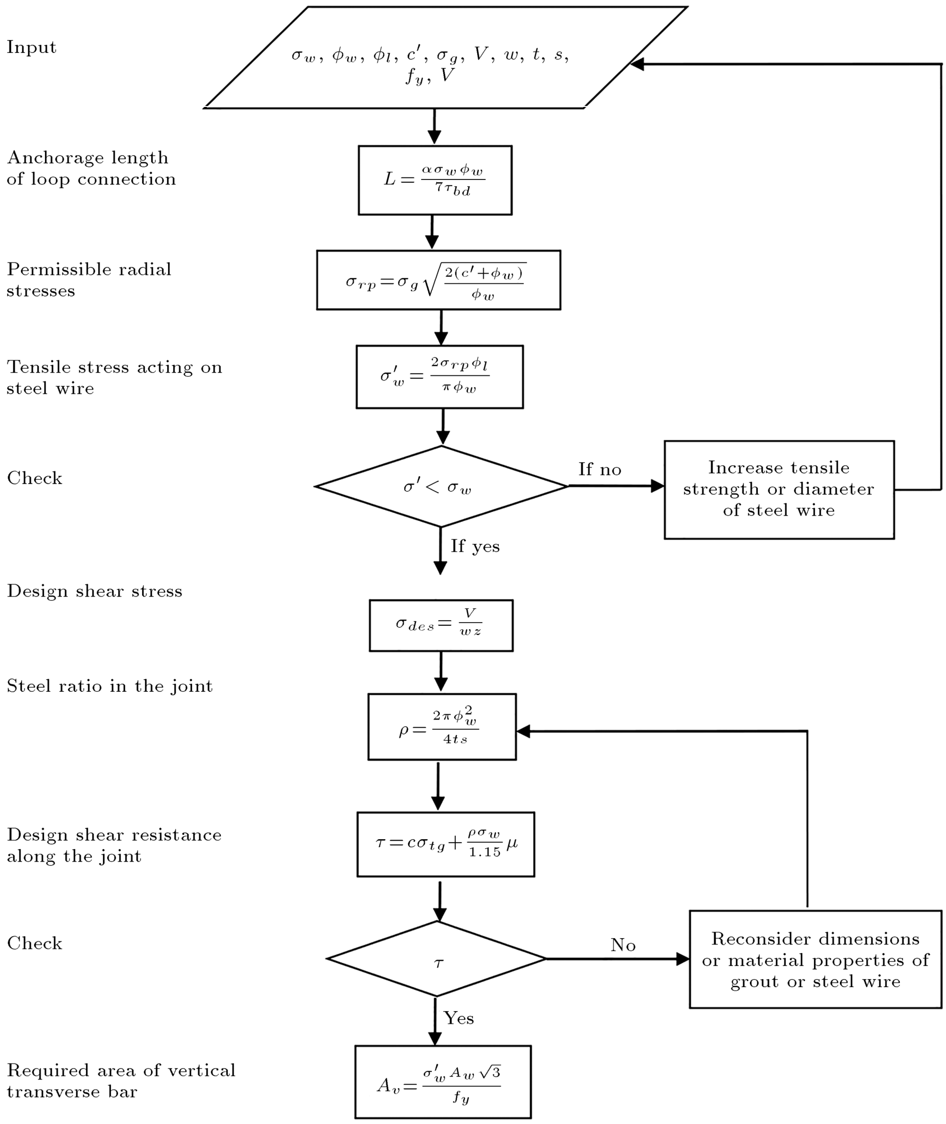

Figure 5. Flow chart depicting the design procedure of the loop connection.

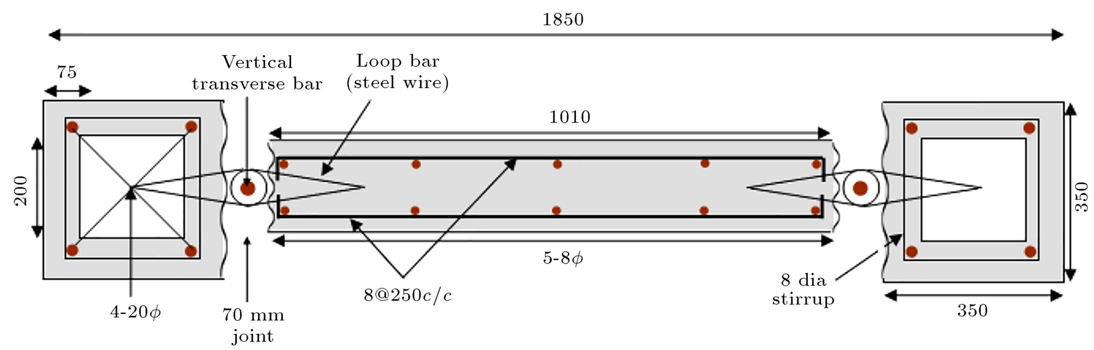

Figure 6. Geometry and structural details of the precast RC wall-column system.

iterations are not carried out; rather, small increments in the load are required to ensure satisfactory results.

Concrete Damage Plasticity (CDP) model well defines the quasi-brittle nature and non-linear behavior of concrete. Literature reports that the CDP model for FEA is able to correctly predict the global behavior of RC structural components, which is governed by non-associated flow law and imparts adequate control for dilatancy, for which the parameter 'dilation angle' is defined in numerical modeling of quasi-brittle elements [34,35]. CDP model is governed by plasticity based on scalar elasticity and continuum mechanics integrated with isotropic compression and tension plasticity [36]. In this modeling approach, hardening variables govern the failure mode, while material and structural characteristics are integrated to yield reliable results. The stress-strain behavior of concrete is defined by strain and damage according to the findings of Mander et al. [37]. Tension stiffening model is adopted for modeling the tension behavior of concrete [38]. Figure 7 depicts the assumed behavior of concrete in uniaxial compression and tension loading. The curves show stress hardening till the yield characterizes linear behavior, thereafter depicting stress softening in the plastic phase. In tension, uniaxial behavior is linearly elastic until the maximum stress corresponding to the initiation of micro-cracking is achieved. Plastic strain may be determined from cracking strain using Eq. (20):

$$\varepsilon_t^{pl} = \varepsilon_t^{ck} - \frac{d_t}{(1-d_t)}\frac{\sigma_t}{E_0}, \tag{20}$$

where ε_t^{pl} = plastic strain; ε_t^{ck} = cracking strain; d_t = function of plastic strain; σ_t = tensile stress; and E_0 = modulus of elasticity.

6.2. Geometrical and material modelling

Three-dimensional continuum solid sections were adopted to model concrete elements, reinforcing bars, and loop bars. Reinforcing bars and loop bars were embedded into the concrete using embedded region constraint. Standard surface-to-surface interactions were defined between the joint grout with precast RC wall and the joint grout with precast RC column. Surface-to-surface contact predicts the appropriate behavior for deformable surfaces. Contact properties were defined in tangential and normal directions. Properties of tangential direction include coefficient of friction, which was defined as 0.3 for finite sliding, while normal behavior was defined with hard contact. To simulate fixity at the base, encastre (fixed boundary condition) was given at the wall base. Meshing was done using eight-nodded linear brick, reduced integration, hourglass control elements. Mesh size was considered in line with the element thickness to prevent mesh distortion. The elastic properties assumed for concrete and steel were density, elastic modulus, and Poisson's ratio, while the plastic properties assumed were eccentricity, dilation angle, viscosity parameter, f_{bo}/f_{co}, and k. Table 2 presents the elastic and plastic properties of concrete and steel. The models were subjected to displacement-controlled lateral loading under non-linear static analysis to undergo inelastic deformation, until the lateral load would degrade to 85% of the peak load.

Table 2. Properties of concrete and steel used in finite element modeling.

Material	Concrete	Rebar
Density (kN/m^3)	24	78.5
Grade (N/mm^2)	30	500
Young's modulus (N/mm^2)	27386	2×10^5
Poisson's ratio	0.19	0.3
Dilation angle (°)	31	—
Eccentricity	0.1	—
f_{bo}/f_{co}	1.16	—
K	0.667	—
Viscosity parameter	0	—

7. Results

The analysis results were derived from the post-processing of the numerical models. The seismic behavior of precast RC wall-columns with loop connection was studied in terms of damage pattern, stress concentration, and lateral load-carrying capacity, and it was compared with those of U-bar connection and conventional monolithic specimen.

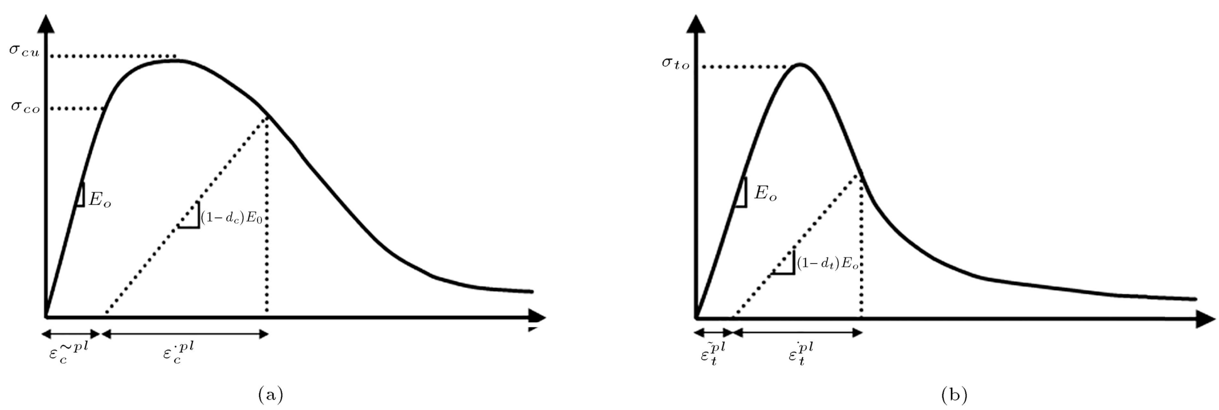

Figure 7. Response of concrete to uniaxial loading in (a) compression and (b) tension.

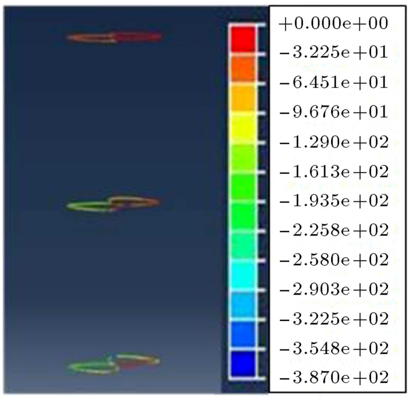

(a)

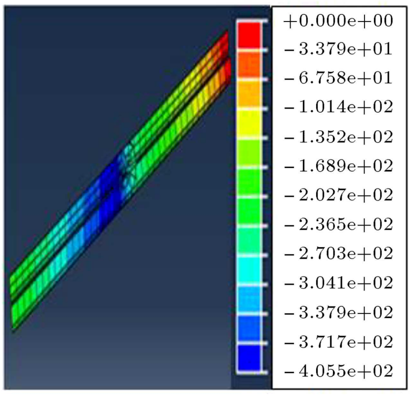

(b)

Figure 8. Stress pattern in (a) loop connection and (b) U-bars.

7.1. Stress concentration

Figure 8 depicts the pattern of stress in connections. It was observed that the U-bars attained maximum stress up to their yield strength (415 N/mm^2), thus indicating failure state. However, the corresponding stress in the steel wire loop connection was 387 N/mm^2, much lower than their yield capacity of 1770 N/mm^2. Loop bars imparted ductility to the system, while the connection using U-bars resulted in stress accumulation in critical regions. All the models demonstrated damage to the bottom of the walls and in the vicinity of the joint, as expected. Figure 9 shows the damage in the analyzed models. Damage pattern in all the three models was similar, with comparatively less damage in the monolithic model than in the precast models.

7.2. Lateral load-carrying capacity

The loop connection demonstrated a lateral load of 319.5 kN at yield limit, after which the model started experiencing stresses in the bottom region and in the joint at the onset of damage. Interestingly, it shall be observed that the steel wire loop connection was designed for a lateral load of 300 kN, up to which the model was intact without any sign of damage. The yield load for the U-bar model was 282.7 kN, while the corresponding value for the monolithic model was 322.5 kN. Obviously, the monolithic model demonstrated higher lateral load resistance due to monolithic system devoid of joints. Figure 10 shows the lateral load versus displacement curves of the analyzed models. According to the numerical analysis, the steel wire loop connection is effective in transferring lateral load between precast panels, while U-bar connection exhibits damage prior to the loop connection using steel wire ropes.

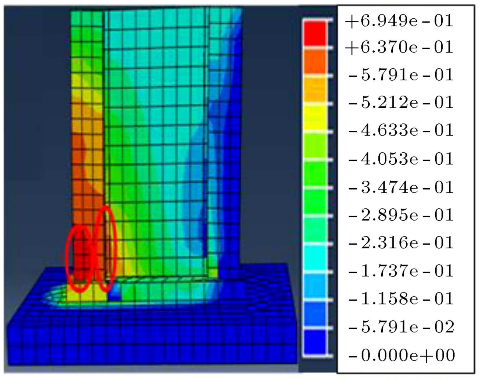

(a)

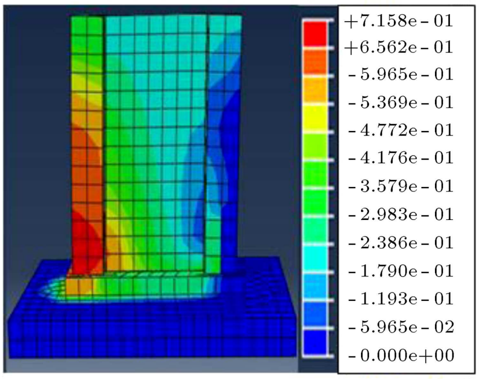

(b)

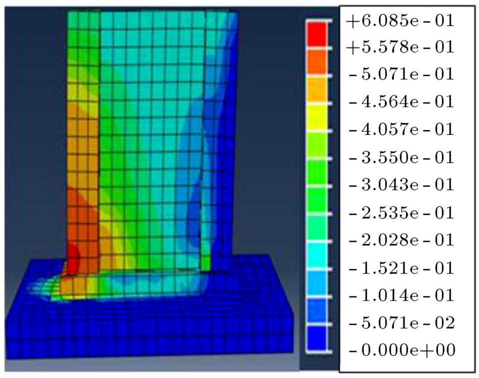

(c)

Figure 9. Damage pattern in tension for (a) model with loop connection, (b) model with U-bar connection, and (c) monolithic model.

7.3. Drift

Precast RC wall-column with the loop connection demonstrated a lateral drift of 2.39% in the ultimate

Table 3. Seismic parameters for different systems.

Seismic parameter	State	Loop connection	U-bar	Monolithic
Lateral load (kN)	Yield	319.54	282.77	322.40
	Maximum	395.14	350.45	412.52
	Ultimate	335.75	297.00	350.64
Displacement (mm)	Yield	15.00	15.00	16.82
	Maximum	26.25	25.50	27.33
	Ultimate	54.02	52.13	60.00
Drift (%)	Yield	0.66	0.66	0.75
	Maximum	1.16	1.13	1.21
	Ultimate	2.39	2.30	2.65

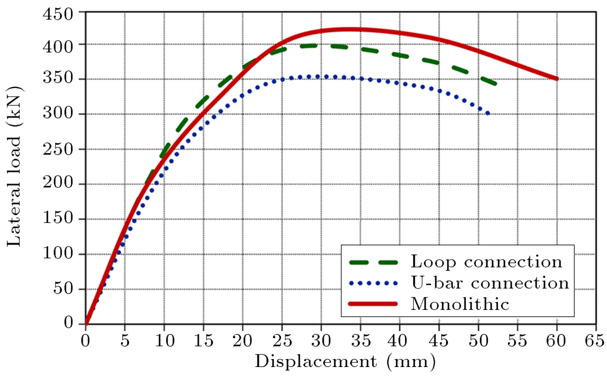

Figure 10. Lateral load versus displacement curves for the analyzed models.

state, while the corresponding value for U-bar connection was 2.30%. The monolithic model exhibited comparatively higher drift (2.65%) due to the absence of the joint. Table 3 summarizes the lateral load and drifts in different limit states for the models analyzed.

8. Conclusion

In spite of the significant popularity of different connection systems, a systematic design formulation of joint connections has not been comprehensively attempted so far. This study aimed to provide the analysis and design methodology of the loop connection for vertical joints between precast components, for which extensive literature survey was done. Loop connection using steel wire ropes is characterized by easy implementation and simple mechanism, facilitating an easy installation process that saves time and manpower, bears high flexibility and strength, along with economy as against the similar connection of U-bar that poses difficulty during practical implications. Advantages of loop connection using steel wire ropes were regarded as an inspiration to formulate a design methodology and safety checks for tensile and shear capacities, which are the main governing factors in the design of connections. Behavior of the loop connection depends on the tension generated in steel wire ropes and shear at the interface of precast panels. Expression for anchorage length was derived based on the bond strength of concrete and maximum possible tension in steel wire ropes. Tensile capacity was a function of anchorage, diameter and strength of steel wire ropes, and diameter of loop. On the other hand, shear capacity was a function of interfacial stresses or friction between grout and precast panels. Tension check was satisfied by limiting the radial stresses in the loop, while shear check was satisfied by limiting the design shear stress along the joint with shear resistance. At higher seismic loads, a vertical interlocking bar in the loop is subjected to horizontal shear and is expected to experience dowel action, for which an expression was given to determine the required transverse steel area. The presented design approach was demonstrated through a design example, where the precast RC wall was connected to end columns through the loop connection designed for a lateral load of 300 kN. The design was validated through a numerical analysis by modeling and analyzing the designed precast RC wall-column system in ABAQUS, which exhibited 319.5 kN yield load, closer to its design load of 300 kN. Further, the loop connection demonstrated better seismic performance than similar U-bar connection in terms of stresses and lateral load-carrying capacity. It is expected that the design approach presented here will be beneficial for practicing engineers and designers to decide on design requirements of the loop connection for vertical joint between precast RC structural components.

Acknowledgment

Authors are grateful to the Director, CSIR- Central Building Research Institute, Roorkee, India for all the support and encouragement during the research work and permitting to publish the paper.

References

1. Casotto, C., Silva, V., Crowley, H., et al. "Seismic

fragility of Italian RC precast industrial structures", *Eng. Struct.*, **94**, pp. 122–136 (2015).

2. Singhal, S., Chourasia, A., Chellappa, S., et al. "Precast reinforced concrete shear walls: State of the art review", *Struct. Concr.*, **20**(3), pp. 886–898 (2019).
3. Fathi, M. and Parvizi, M. "Experimental and numerical study on proposed T-form semi-precast moment-resisting concrete connections", *Sci. Iran.*, **28**(1), pp. 85–95 (2019).
4. Fathi, M., Parvizi, M., Karimi, J., et al. "Experimental and numerical study of a proposed moment-resisting connection for precast concrete frames", *Sci. Iran.*, **25**(4), pp. 1977–1986 (2018).
5. Fan, J.J., Wu, G., Feng, D.C., et al. "Seismic performance of a novel self-sustaining beam-column connection for precast concrete moment-resisting frames", *Eng. Struct.*, **222**, p. 111096 (2020).
6. Chourasia, A., Kajale, Y., Singhal, S., et al. "Seismic performance assessment of two-storey precast reinforced concrete building", *Struct. Concr.*, **21**(5), pp. 2011–2027 (2020).
7. Ashok, M.K., Thangam, J.S., and Govindharajan, V. "Experimental investigation of precast horizontal wall panel connection using reinforcement by push off test", *Int. J. Sci. Res. Dev.*, **4**(3), pp. 2321–0613 (2016).
8. Pramodh, R., Shripriyadharshini, V., and Vidjeapriya, R. "Shear behavior of horizontal joints between precast panels", *Asian J. Civ. Eng.*, **19**(6), pp. 651–662 (2018).
9. El-desoqi, M., Ehab, M., and Salem, H. "Progressive collapse assessment of precast reinforced concrete beams using applied element method", *Case Stud. Constr. Mater.*, **13**, p. e00456 (2020).
10. Chourasia, A. and Gupta, S. "Influential parameters for headed bars in RC beam-column joint", *Curr. Sci.*, **116**(10), pp. 1666–1673 (2019).
11. Singhal, S., Chourasia, A., and Parashar, J. "Anchorage behaviour of headed bars as connection system for precast reinforced concrete structural components", *Structures*, **27**, pp. 1405–1418 (2020).
12. Sritharan, S., Aaleti, S., Henry, R.S., et al. "Precast concrete wall with end columns (PreWEC) for earthquake resistant design", *Earthquake Eng. Struct. Dyn.*, **44**(12), pp. 2075–2092 (2015).
13. Brunesi, E., Peloso, S., Pinho, R., et al. "Cyclic testing and analysis of a full-scale cast-in-place reinforced concrete wall-slab-wall structure", *Bull. Earthquake Eng.*, **16**(10), pp. 4761–4796 (2018).
14. Vaghei, R., Hejazi, F., Firoozi, A.A., et al. "Performance of loop connection in precast concrete walls subjected to lateral loads", *Int. J. Civ. Eng.*, **17**(3), pp. 397–426 (2019).
15. Joergensen, H.B. and Hoang, L.C. "Tests and limit analysis of loop connections between precast concrete elements loaded in tension", *Eng. Struct.*, **52**, pp. 558–569 (2013).
16. Jørgensen, H.B. and Hoang, L.C. "Strength of loop connections between precast bridge decks loaded in combined tension and bending", *Struct. Eng. Int.*, **25**(1), pp. 71–80 (2015).
17. Rossley, N., Aziz, A.A., Chew, H., et al. "Behaviour of vertical loop bar connection in precast wall subjected to shear load", *Aus. J. Basic Appl. Sci.*, **8**(1), pp. 370–380 (2014).
18. Araújo, D., Curado, M.C., and Rodrigues, P.F. "Loop connection with fibre-reinforced precast concrete components in tension", *Eng. Struct.*, **72**, pp. 140–151 (2014).
19. Sørensen, J.H., Hoang, L.C., Olesen, J.F., et al. "Tensile capacity of loop connections grouted with concrete or mortar", *Mag. Concr. Res.*, **69**(17), pp. 892–904 (2017).
20. Biswal, A., Prasad, A.M., and Sengupta, A.K. "Study of shear behavior of grouted vertical joints between precast concrete wall panels under direct shear loading", *Struct. Concr.*, **20**(2), pp. 564–582 (2019).
21. Jøgensen, H.B., Bryndom, T., Larsen, M., et al. "Load carrying capacity of shear wall t-connections reinforced with high strength wire ropes", *Fib Symposium: Performance-Based Approaches for Concrete Structures*, Cape Town, South Africa (2016).
22. Peng, Y.Y., Qian, J.R., and Wang, Y.H. "Cyclic performance of precast concrete shear walls with a mortar-sleeve connection for longitudinal steel bars", *Mater. Struct.*, **49**(6), pp. 2455–2469 (2016).
23. Qiong, Y., Kun, X., Zhiyuan, X., et al. "Seismic behavior of precast shear walls with vertical reinforcements overlap grouted in constraint sleeve", *Revista Tecnica de la Facultad de Ingenieria Universidad del Zulia*, **39**, pp. 207–217 (2016).
24. Li, J., Wang, Y., Lu, Z., et al. "Experimental study and numerical simulation of a laminated reinforced concrete shear wall with a vertical seam", *Appl. Sci.*, **7**(6), pp. 1–19 (2017).
25. Sun, J., Qiu, H., and Jiang, H. "Experimental study and associated mechanism analysis of horizontal bolted connections involved in a precast concrete shear wall system", *Struct. Concr.*, **20**(1), pp. 282–295 (2019).
26. Wang, W., Li, A., and Wang, X. "Seismic performance of precast concrete shear wall structure with improved assembly horizontal wall connections", *Bull. Earthquake Eng.*, **16**(9), pp. 4133–4158 (2018).
27. Guo, W., Zhai, Z., Cui, Y., et al. "Seismic performance assessment of low-rise precast wall panel structure with bolt connections", *Eng. Struct.*, **181**, pp. 562–578 (2019).
28. Li, X., Kurama, Y.C., and Wu, G. "Experimental and numerical study of precast posttensioned walls with yielding-based and friction-based energy dissipation", *Eng. Struct.*, **212**, pp. 1–19 (2020).
29. British Standard, *Structural Use of Concrete-Part 1. Code of Practie for Design and Construction*, B.S. 8110, London, UK (1997).

30. DIN, *Concrete and Reinforced Concrete Structures, Design and Construction*, DIN 1045, Berlin, Germany (1978).

31. Basler and Witta, *Basics of Structural Connections in Prefabrication*, Wildegg, Switzerland (1966).

32. Nielsen, M.P. and Hoang, L.C. *Limit Analysis and Concrete Plasticity*, Florida, USA: CRC Press (2016).

33. CEN (European Committee for Standardization), *Design of Concrete Structures-Part 1-1, Eurocode 2*, Brussels, Belgium: CEN (2004).

34. Li, X.X.L. "Parametric study on numerical simulation of missile punching test using concrete damaged plasticity (CDP) model", *Int. J. of Impact Eng.*, **144**, p. 103652 (2020).

35. Raza, A. and Ahmad, A. "Numerical investigation of load-carrying capacity of GFRP-reinforced rectangular concrete members using CDP model in ABAQUS", *Adv. Civ. Eng.*, **2019**, pp. 1–21 (2019).

36. Lubliner, J., Oliver, J., Oller, S., et al. "A plastic-damage model for concrete", *Int. J. Solids Struct.*, **25**(3), pp. 229–326 (1989).

37. Mander, J.B., Priestley, M.J., and Park, R. "Theoretical stress-strain model for confined concrete", *J. Struct. Eng.*, **114**(8), pp. 1804–1826 (1988).

38. Nayal, R. and Rasheed, H.A. "Tension stiffening model for concrete beams reinforced with steel and FRP bars", *J. Mater. Civ. Eng.*, **18**(6), pp. 831–841 (2006).

Biographies

Shubham Singhal is a PhD Scholar at CSIR- Central Building Research Institute, Roorkee under Academy of Scientific & Innovative Research (AcSIR). His research interests are precast technology, seismic vulnerability, and earthquake-resistant design of structures. He has worked extensively on testing methods, numerical analysis, and development of design methodology for structural systems.

Ajay Chourasia is a Senior Principal Scientist at CSIR-Central Building Research Institute, Roorkee (India), having a professional experience of over 25 years. His area of specialization is structural engineering and earthquake engineering/earthquake resistant design. He has published numerous research papers in various international and national journals and conferences, focusing primarily on structural health monitoring, building materials, seismic behavior of masonry buildings, precast technology, seismic vulnerability, and strengthening/retrofitting of buildings.

Yogesh Kajale is the Vice President (Planning and Design) at BG Shirke Construction Technology Pvt. Ltd., Pune. He has vast professional experience in the field of designing and construction of precast reinforced concrete buildings. He is a design expert in joint connections between precast reinforced concrete structural components.